JBC RESEARCH ARTICLE

Rhodoquinone-dependent electron transport chain is essential for *Caenorhabditis elegans* survival in hydrogen sulfide environments

Received for publication, February 28, 2024, and in revised form, July 29, 2024 Published, Papers in Press, August 22, 2024,
https://doi.org/10.1016/j.jbc.2024.107708

Laura Romanelli-Cedrez[1,*], **Franco Vairoletti**[1,2], **and Gustavo Salinas**[1,3,*]

From the [1]*Worm Biology Lab, Institut Pasteur de Montevideo, Montevideo, Uruguay;* [2]*Laboratorio de Química Farmacéutica, Departamento de Química Orgánica, and* [3]*Departamento de Biociencias, Facultad de Química, Universidad de la República, Montevideo, Uruguay*

Reviewed by members of the JBC Editorial Board. Edited by Ursula Jakob

Hydrogen sulfide (H_2S) has traditionally been considered an environmental toxin for animal lineages; yet, it plays a signaling role in various processes at low concentrations. Mechanisms controlling H_2S in animals, especially in sulfide-rich environments, are not fully understood. The main detoxification pathway involves the conversion of H_2S into less harmful forms, through a mitochondrial oxidation pathway. The first step of this pathway oxidizes sulfide and reduces ubiquinone (UQ) through sulfide-quinone oxidoreductase (SQRD/SQOR). Because H_2S inhibits cytochrome oxidase and hence UQ regeneration, this pathway becomes compromised at high H_2S concentrations. The free-living nematode *Caenorhabditis elegans* feeds on bacteria and can face high sulfide concentrations in its natural environment. This organism has an alternative ETC that uses rhodoquinone (RQ) as the lipidic electron transporter and fumarate as the final electron acceptor. In this study, we demonstrate that RQ is essential for survival in sulfide. RQ-less animals (*kynu-1* and *coq-2e* KO) cannot survive high H_2S concentrations, while UQ-less animals (*clk-1* and *coq-2a* KO) exhibit recovery, even when provided with a UQ-deficient diet. Our findings highlight that *sqrd-1* uses both benzoquinones and that RQ-dependent ETC confers a key advantage (RQ regeneration) over UQ in sulfide-rich conditions. *C. elegans* also faces cyanide, another cytochrome oxidase inhibitor, whose detoxification leads to H_2S production, *via cysl-2*. Our study reveals that RQ delays killing by the HCN-producing bacteria *Pseudomonas aeruginosa* PAO1. These results underscore the fundamental role that RQ-dependent ETC serves as a biochemical adaptation to H_2S environments, and to pathogenic bacteria producing cyanide and H_2S toxins.

Hydrogen sulfide (H_2S) has long been regarded as toxic to many animals due to inhibition of cellular respiration (1). Recent research in mammals has shown that H_2S can function as a signaling molecule at low concentrations (2), renewing interest in H_2S research. Other animal lineages, such as invertebrates that thrive in marine sediments, can cope with environmental hypoxia and sulfide-rich environments (3–6). The molecular mechanisms that underlie the control of H_2S levels differ in different animal lineages and are not fully understood.

In animals, the main detoxification pathway of H_2S involves its conversion into less toxic forms, through a mitochondrial oxidation pathway (7). The first enzyme involved in this pathway is sulfide:quinone oxidoreductase (SQRD/SQOR), which catalyzes the oxidation of H_2S to less toxic low molecular weight persulfides and the reduction of ubiquinone (UQ). The persulfides are further oxidized to sulfate in subsequent reactions catalyzed by persulfide dioxygenase, sulfur transferase, and sulfite oxidase (7–9). Because SQRD transfers electrons to the electron transport chain (ETC) and H_2S can lead to inhibition of ETC complex IV (cytochrome c oxidase), this pathway may be insufficient to withstand high H_2S concentrations. Invertebrates living in sulfide-rich environments, such as mussels and nematodes, have multiple SQRD/SQOR genes and additional mechanisms to deal with H_2S, including association with episymbiont and endosymbiont bacteria (5).

Caenorhabditis elegans inhabits the soil, where it feeds on bacteria and encounters various environmental challenges, including bacteria that produce sulfide and/or cyanide (10–12). Indeed, cyanide poisoning is a killing mechanism used by *C. elegans* pathogens, such as *Pseudomonas* spp (10). These toxins may have imposed selective pressures leading to specific biochemical adaptations. Indeed, the cysteine synthase homologs CYSL-1 and CYSL-2 conform to a cyanide-assimilation pathway. CYSL-2 is a cyanoalanine synthase that catalyzes the conversion of cyanide and cysteine into β-cyanoalanine and H_2S, lowering cellular cyanide levels (13). The resultant H_2S is detoxified mainly by the sulfide oxidation pathway. CYSL-1, in turn, is an enzyme that in some lineages catalyzes the conversion of H_2S and O-acetylserine to cysteine and acetate, but in *C. elegans* functions as a sulfide sensor (11, 14).

In the presence of H_2S, CYSL-1 interacts with the O_2-sensing hydroxylase EGL-9 (14, 15) to promote a HIF-induced response to H_2S and HCN, which leads to an increased expression of *sqrd-1 and cysl-2* (16, 17). This suggests that this hypoxia-independent

* For correspondence: Laura Romanelli-Cedrez, lromanelli@pasteur.edu.uy; Gustavo Salinas, gsalinas@pasteur.edu.uy, gsalin@fq.edu.uy.

HIF-1 response in *C. elegans* evolved to withstand high concentrations of naturally occurring H_2S and HCN. It has been proposed that *cysl-1* and *cysl-2* genes would have been co-opted to protect this lineage against cyanogenic toxins (13). More recently, a HIF-1-independent sulfide detoxification mechanism involving the SKN-1/NRF-2 transcription factor has been described, through CYSL-1 and RHY-1 (18).

A key biochemical adaptation of *C. elegans* and some other animal lineages that face hypoxia is the existence of an alternative mitochondrial ETC in which rhodoquinone (RQ), and not UQ, serves as the lipidic electron transporter (19, 20). In this alternative ETC, complex I reduces rhodoquinone (RQ) to rhodoquinol (RQH_2). RQH_2 is oxidized back to RQ by complex II, which reduces fumarate to succinate, catalyzing the reverse reaction to the canonical activity of complex II (succinate dehydrogenase) (21, 22). In this abbreviated alternative ETC, fumarate, not oxygen, is the final electron acceptor (22). Because both H_2S and HCN can lead to inhibition of complex IV, this alternative ETC would confer an advantage to *C. elegans* survival against these toxins. *C. elegans* mutants unable to synthesize RQ are more sensitive to cyanide than mutants unable to synthesize UQ (23).

The structural difference between RQ and UQ is a single substituent at position 2 of the benzoquinone ring (an amine group in RQ vs a methoxy group in UQ). This change impacts the standard reduction potential (E^o). The E'^o of RQ/RQH_2 couple (rhodoquinone/rhodoquinol) has been reported to be −30 or −63 mV (bound to chromatophores or pure in a hydroalcoholic solution, respectively) (24). Because RQ/RQH_2 E'^o is higher than that of NAD^+/NADH couple (−320 mV) and lower than that of fumarate/succinate couple (+30 mV), it allows fumarate to be readily reduced by RQH_2, and RQ by NADH. In contrast, the E'^o of UQ/UQH_2 couple (ubiquinone/ubiquinol) is +50 mV or +43 mV (bound to chromatophores or pure, respectively) (24), higher than that of the succinate/fumarate couple, thus thermodynamically favoring succinate oxidation. Importantly, RQ is synthesized by nematodes, bivalves, and annelids, which are the animal lineages more abundant in hypoxia and sulfide-rich environments (3–6).

We reasoned that the canonical sulfide detoxification pathway, which oxidizes sulfide and reduces ubiquinone may be compromised at high sulfide concentrations due to inhibition of complex IV, while the RQ-dependent ETC would be fully functional in sulfide-rich conditions. Although UQ-complex II in reverse has been implicated in sulfide oxidation *in vitro* (25), the redox potential of RQ-complex II allows sulfide oxidation over a broader range of concentrations. In the present work, we demonstrate that RQ is essential for survival at high sulfide concentrations. Mutants unable to synthesize RQ are more susceptible to H_2S than mutants unable to synthesize UQ. In addition, we showed that besides sulfide:quinone oxidoreductase *sqrd-1*, previously reported to be essential in *C. elegans* sulfide response, Y9C9A.16 (from now on *sqrd-2*), thought to be a pseudogen, is expressed and plays a marginal role in the recovery response to sulfide. Finally, we show that RQ has a role in the presence of the HCN-producing bacteria *Pseudomonas aeruginosa* PAO1.

Results

We hypothesize that RQ would be the key benzoquinone in sulfide detoxification, accepting electrons from H_2S through SQRD/SQOR. This would confer the advantage of transferring electrons independently of complex IV. SQRD/SQOR uses FAD as a cofactor to transfer electrons from H_2S to UQ in the canonical mechanism. Because the standard reduction potential of FAD attached to the SQRD/SQOR is approximately −123 mV (26); it would be thermodynamically possible to transfer electrons from FAD to RQ, but whether the active site of *C. elegans* SQRD/SQORs can accommodate RQ is not known.

C. elegans *possess two sulfide:quinone oxidoreductases that accommodate both RQ and UQ*

C. elegans possesses two SQRD/SQOR genes, both with approximately 45% identity to human SQOR (alignment shown in Fig. S1). One of them, *sqrd-1*, has been previously characterized and involved in sulfide response (11), while the other, *Y9C9A.16*, was initially proposed to be a pseudogen (quoted in (11)). Interestingly, other nematode, platyhelminth, and mollusk lineages also possess two SQRD genes (Fig. S1). We found that *Y9C9A.16* is expressed in *C. elegans*, yielding an mRNA of the expected size according to the gene model (Fig. S2).

We then examined *in silico* whether *C. elegans* SQRD-1 and SQRD-2 would be able to accommodate RQ and/or UQ at the benzoquinone-binding site. Both quinones bind similarly to *C. elegans* SQRD-1 and SQRD-2. There are no clashes that would impede the binding of either benzoquinones to either enzyme. Binding free energy estimated through GBVI and KDeep are negative and suggest a favorable interaction (Table 1). Both quinones establish hydrogen bonds through the carbonyl moieties with Trp455 and Lys438 (numbering corresponding to SQRD-1 isoform a, highlighted in cyan in Fig. S1) in both enzyme models, being the main polar interactions with the enzyme (Fig. 1, *A* and *B*). All the other interactions are hydrophobic and thus little affected by the presence of a methoxy or amino substituent. Furthermore, both quinones are located near the FAD cofactor in the holoenzyme, within a distance compatible

Table 1
Binding energy of RQ and UQ in complex with SQRD-1 and SQRD-2

Benzoquinone	SQRD-1 binding energy (kcal/mol)	SQRD-2 binding energy (kcal/mol)
Ubiquinone	−7.4183 (GBVI)/−6.70 ± 0.96 (KDeep)	−7,4253 (GBVI)/−6.63 ± 0.53
Rhodoquinone	−6.9301 (GBVI)/−6.76 ± 0.87 (KDeep)	−7,1337 (GBVI)/−7.45 ± 0.30 (KDeep)

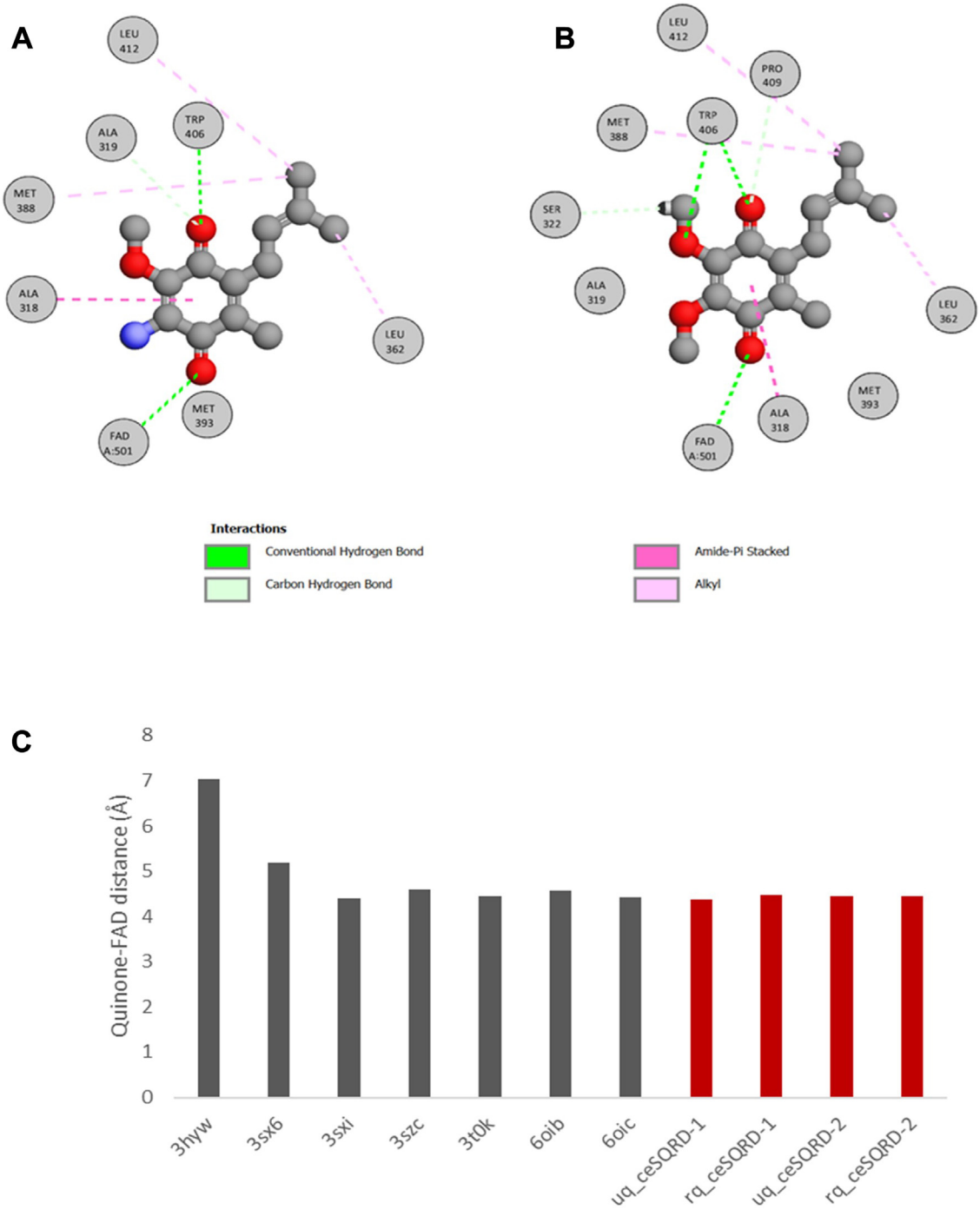

Figure 1. *C. elegans* SQRD-1 can accommodate both benzoquinones, UQ and RQ, at its active site. *A*, interaction diagram of RQ docked in the homology model of SQRD-1. *B*, interaction diagram of UQ docked in the homology model of SQRD-1. *C*, comparison of the distance between the quinone ring and the imidic nitrogen of FAD in sulfide:quinone oxidoreductase structures deposited at PDB (grey) and the quinones ubiquinone (uq) and rhodoquinone (rq) docked in the homology models of *C.elegans* SQRD-1 and SQRD-2 (*red*). 3HYW: *Aquifex aeolicus* SQRD in complex with decylubiquinone; 3SX6: *Acidithiobacillus ferrooxidans* SQRD complexed with decylubiquinone, 3SXI: *Acidithiobacillus ferrooxidans* SQRD complexed with decylubiquinone, 3SZC: *Acidithiobacillus ferrooxidans* SQRD in complex with gold (I) cyanide, 3t0K: *Acidithiobacillus ferrooxidans* SQRD with bound trisulfide and decylubiquinone, 6OIB: human SQRD in complex with coenzyme Q, 6OIC: human SQRD in complex with coenzyme Q.

with electron transfer reactions and within the range of quinone/FAD distance in PDB deposited structures (Fig. 1*C*). The stability of the modeled SQRD complexes with RQ and UQ was tested using equilibrium molecular dynamics. The simulations showed that all four models equilibrated and remained stable at least for 50 ns. The secondary structure of the homology models was kept during the simulation and the complexes evolved similarly when compared to the crystal structure 6oic (also dynamized under the same conditions). UQ and RQ were kept in the quinone site of SQRD-1 and SQRD-2 and within a distance compatible with an electron transfer reaction during the simulation. Input files

and evolution of protein RMSD, quinone-FAD distance, and total energy during simulation time for each complex are available upon request.

Interestingly, the gene models of *sqrd-1* and *sqrd-2* predict alternative transcripts and protein isoforms. Six isoforms are predicted for SQRD-1(a-f) and two for SQRD-2 (a and b) (Fig. S1). All isoforms have the quinone binding site; however, the FAD-binding domain and the sulfide binding are absent in SQRD-1d and SQRD-1e isoforms. SQRD-1b and SQRD-2b isoforms possess N-terminal extensions, whose functional significance is yet to be characterized. In addition, three SQRD-1 isoforms (a, e and f) possess a 48-amino acid insertion that, according to modeling, would form an external loop not affecting the canonical folding of the protein.

We examined *sqrd-1(tm3378)* and *sqrd-2(ok3440)* mutant strains in the presence of sulfide in the liquid phase, using motility as a readout with *WMicrotracker ONE* (Fig. 2). Because the *WMicrotracker ONE* is an open system, the sulfide concentration in solution decreases over time. We observed a decrease from 1.5 mM to 0 mM in 3 h and from 0.5 mM to 0 in 2 h (Fig. S3). The *sqrd-1* mutant strain (*sqrd-1(tm3378)*) is more sensitive to sulfide than the wild-type N2 strain (Fig. 2). The *sqrd-1(tm3378)* strain initially decreased its motility similarly to N2; however, once sulfur concentration decreased, the motility recovery of *sqrd-1(tm3378)* was slower than that of the N2 strain (Fig. 2, *A* and *B*). This could be due to an induced expression of *sqrd-1* in sulfide-rich conditions, resulting in sulfide detoxification. In addition, the sulfide oxidation pathway leads to sulfur species that mediate sulfide signaling, contributing to redox homeostasis and thus organismal wellness ((27). In contrast to the *sqrd-1* mutant strain, the recovery of *sqrd-2* mutant strain (*sqrd-2(ok3440)*) was slightly earlier than that of the N2 strain (Fig. 2, *A* and *B*). The results obtained suggest that, in addition to the previously described SQRD-1, SQRD-2 is also involved in the organism's response to sulfide.

The *sqrd-1(tm3378)* and *sqrd-2(ok3440)* mutant strains were then examined in NGM-plates with food in the presence of gaseous sulfide concentration and incubation time that paralyzed but not kill the worms. After 4 h of exposure to gaseous sulfide at a concentration that transiently paralyzed wild-type N2 animals and *sqrd-1* mutants, *sqrd-2* mutants were crawling normally, consistent with the early recovery observed in a liquid phase (Fig. 2, *C* and *D*).

RQ is essential for survival in sulfide

We next examined the relevance of RQ and UQ in H_2S response. Since KYNU-1 is essential for RQ synthesis (28), we tested the *kynu-1(tm4924)* loss-of-function mutant for its response to H_2S. This strain was highly sensitive to H_2S, compared to the wild-type strain (Fig. 3, *A* and *B*). Importantly, almost all *kynu-1(tm4924)* animals died after 3 and 20 h in H_2S at 1.5 mM (Fig. 3*C*), whereas most wild-type worms were alive under these conditions. In contrast to *kynu-1(tm4924)*, the null-mutant strain *clk-1(qm30)*, unable to synthesize UQ, showed a complete motility recovery as the wild-type when H_2S concentration decreased. Yet, the drop and recovery of motility in this mutant was more pronounced than that of the wild-type strain (Fig. 3, *A* and *B*). The same effect was observed with 0.5 mM of H_2S (Fig. S4).

Additionally, null-mutant strains *kynu-1(tm4924)* and *clk-1(qm30)* were examined in the presence of gaseous sulfide. In concordance with the results obtained in liquid media, the *kynu-1(tm4924)* mutant strain was highly sensitive to H_2S compared to both the wild-type and *clk-1(qm30)* mutant strains. Specifically, while most wild-type and *clk-1(qm30)* worms were alive under these conditions, only 25% of *kynu-1(tm4924)* worms survived (Fig. 3*D*).

These results indicate that in these sulfide-rich conditions, RQ was even more important than endogenous UQ for motility recovery and survival. Because the OP50 diet contains bacterial UQ, we then examined the sulfide response of the *clk-1(qm30)* mutant strain fed during 20 h with OP50 and afterwards with the UQ-less *Escherichia coli* strain GD1 (feeding with GD1 from L1 results in larval arrest). The *clk-1* mutant strain fed with UQ-less diet showed a motility recovery similar to the results obtained using OP50 as food (Fig. 3*E*). These results indicate that RQ is more relevant than UQ in the sulfide response, independently of the source of UQ.

COQ-2 is essential for RQ and UQ biosynthesis (29). Organisms that synthesize RQ possess two isoforms of this enzyme (COQ-2A and COQ-2E), derived from mutually exclusive alternative splicing (29). COQ-2E, which is absent in organisms that do not synthesize RQ, has been shown to be essential for RQ biosynthesis. We examined the two COQ-2 isoforms mutants under sulfide-rich conditions. Consistent with the results obtained with *kynu-1(tm4924)* and *clk-1(qm30)* mutant strains, the deletion mutant in exon 6e (*coq-2Δ6e*), was more sensitive to H_2S than both the wild-type and the COQ-2a mutant strains (Fig. S5).

We then performed the genetic rescue of the wild-type phenotypes expressing the *kynu-1* wild-type allele in the *kynu-1(tm4924)* mutant strain. We analyzed survival and progeny under gaseous H_2S exposure. Similar to the wild-type strain, all worms of the transgenic strain survived under sulfide-rich conditions, in contrast to the *kynu-1(tm4924)* mutant animals (Fig. 4*A*). Furthermore, the expression of the *kynu-1* wild-type allele in the *kynu-1(tm4324)* mutant strain restored the progeny size in H_2S, confirming the role of KYNU-1 in the H_2S response (Fig. 4, *B* and *C*).

Altogether, these results indicate that RQ is required for the organismal response to sulfide exposure.

RQ plays a role in the organismal response to pathogenic bacteria

We examined the RQ deficient mutant strains in response to *P. aeruginosa PAO1*, a bacterial strain that has been described to paralyze and kill the worm by cyanide production (10, 12). Cyanide detoxification leads to sulfide generation through CYSL-2 (11). Furthermore, it has been shown that RQ confers an advantage for cyanide recovery (23). Therefore, RQ could confer an advantage to *C. elegans* response to *P. aeruginosa PAO1*. We found that the *kynu-1(tm4924)* strain

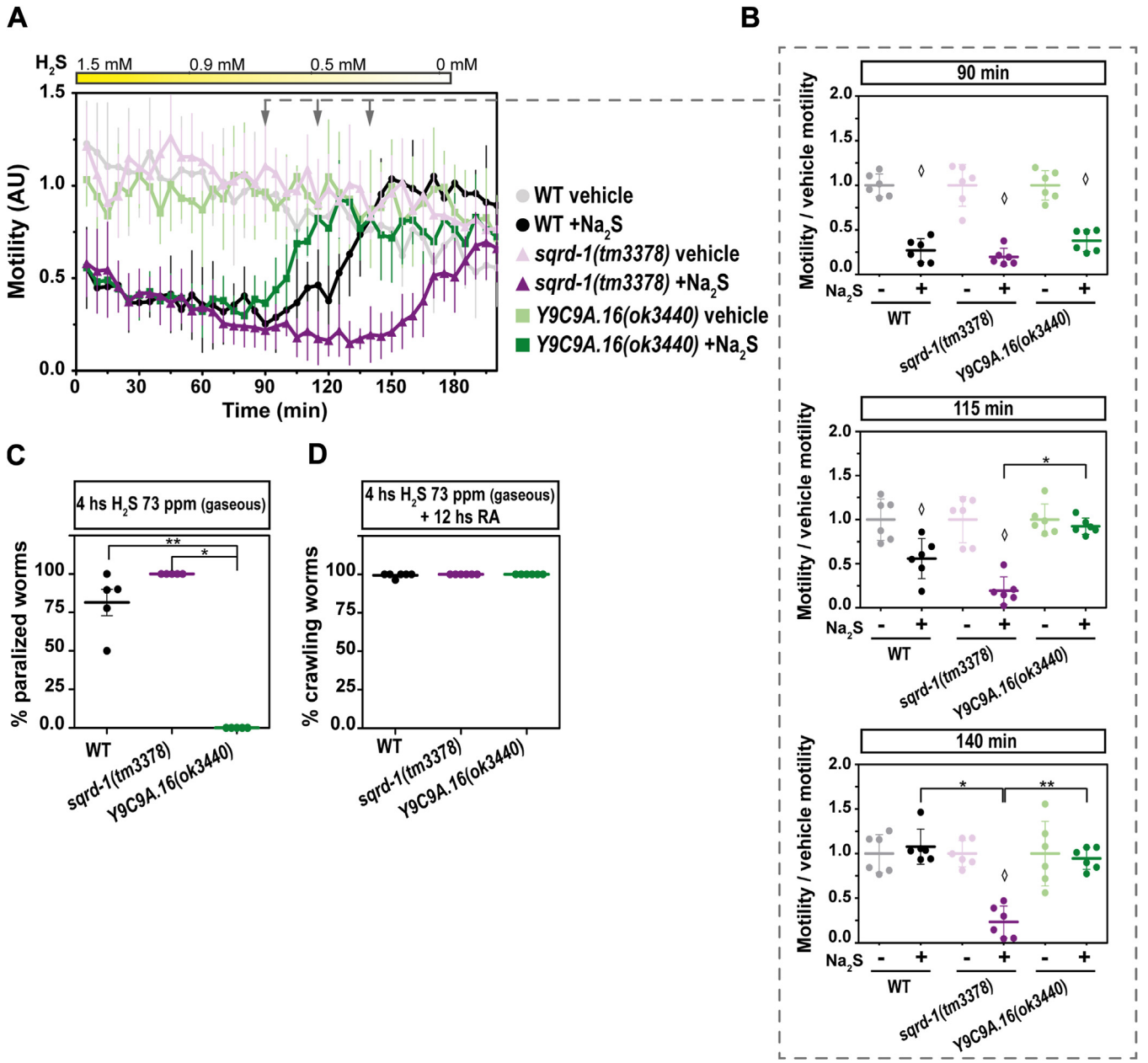

Figure 2. *C. elegans* possesses two sulfide quinone oxidoreductases. The motility parameter refers to the motility of a population of individuals in liquid media and was measured using the infrared tracking device *WMicrotracker*. *A*, motility of *sqrd-1(tm3378)* and *Y9C9A.16(ok3440)* mutants and wild-type (WT) strains in the presence (+Na_2S) or absence (vehicle) of sodium sulfide (Na_2S) solution. Each point indicates the motility average of 6 wells (relative to the habituation, see methods) measured every 5 min for 200 min. The graph corresponds to a representative experiment with 6 wells per condition per strain (approximately 80 worms per well). Error bars indicate the standard deviation. At least three biological replicates were performed for each worm strain (all the replicates and raw data are included in Supporting information). The *yellow* rectangle represents the decrease with time of the sulfide concentration in solution from 1.5 mM (50 ppm of sulfide) as initial concentration in the wells. Arrows represent the three time points shown in part B). AU: arbitrary units. *B*, For each strain (*sqrd-1(tm3378)*, *Y9C9A.16(ok3440)* and WT), the motility in the presence (+) or absence (–) of sulfide (Na_2S) was normalized to the mean of the motility in the absence of Na_2S. Each data point represents the normalized motility of each one of the 6 wells for each condition (with or without Na_2S). Different graphs correspond to the time points of 90, 115 and 140 min of incubation. Kruskal-Wallis test were performed (115 min p = 2.4E-5 and 140 min p = 2.5E-3) was performed, followed by Dunn´s *post hoc* test. ANOVA test (90 min p = 4.6E-15) was performed, followed by Tuckey pairwise. Asterisks indicate statistical differences between the strains indicated (115 min *p = 2.5E-3 and 140 min *p = 4.8E-4, **p = 1.1E-2). Diamonds indicate statistical differences between sulfide and control vehicle (without sulfide) for each strain. All the p values obtained with statistical tests are shown in Supporting information. *C* and *D*, Gravid adults (24–30 h post L4) were exposed to a sulfide atmosphere (73 ppm) for 4 h, followed by 12 h of room air (RA). The number of paralyzed animals was scored immediately after the sulfide incubation (*C*). The number of crawling animals was scored after 12 hs in RA after sulfide incubation (*D*). Each data point represents the percentage of paralyzed or crawling worms obtained in independent experiments (∼30 animals per replicate were used). WT, wild-type N2 strain. Error bars represent the standard deviation. Kruskal-Wallis test was performed (p = 1.8E-3) and subsequent Dunn´s *post hoc* test. Asterisks indicate statistical differences (*p = 4.0E-4 and **p = 4.0E-2).

was slightly more sensitive to the pathogenic bacteria than the wild-type strain (Fig. 5). In contrast to *kynu-1(tm4924)*, the *clk-1(qm30)* mutant strain was similar to wild-type worms in response to the pathogenic bacteria PAO1 for 3 h (Fig. 5). Further exposure to this bacterial strain, led to motility decrease for all strains. Consistent with these results, the *coq-*

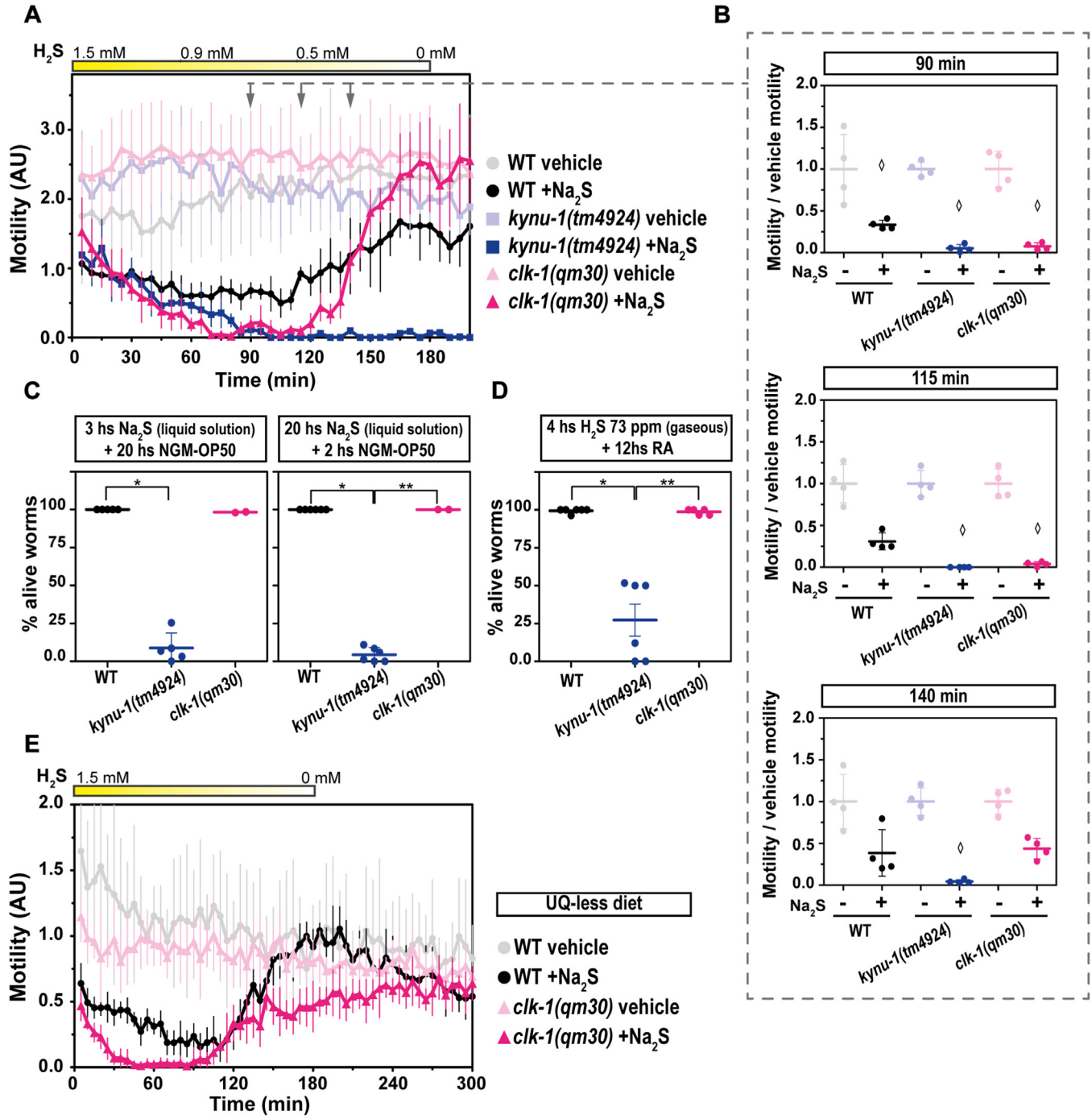

Figure 3. The rhodoquinone-deficient mutant strain (*kynu-1(tm4924)*) does not recover from sulfide challenge in contrast to the ubiquinone-deficient mutant strain (*clk-1(qm30)*). The motility parameter refers to the movement of a population of individuals in liquid media and was measured using the infrared tracking device *WMicrotracker*. *A*, Motility of *kynu-1(tm4924)* and *clk-1(qm30)* mutants and wild-type (WT) strains in the presence (+Na_2S) or absence (vehicle) of a sodium sulfide (Na_2S) solution. Each point indicates the motility average of 4 wells (relative to the habituation, see methods) measured every 5 min for 200 min. The graph corresponds to a representative experiment with 4 wells per condition per strain (approximately 80 worms per well). Error bars indicate the standard deviation. At least three biological replicates were performed for each worm strain (all the replicates and raw data are included in Supporting information). The yellow rectangle represents the decrease of the sulfide concentration in solution from 1.5 mM (50 ppm of sulfide). Arrows represent the three time points shown in part B). AU: arbitrary units. *B*, For each strain (*kynu-1(tm4924)*, *clk-1(qm30)* and WT), the motility in the presence (+) or absence (–) of sulfide (Na_2S) was normalized to the mean of the motility in the absence of Na_2S. Each data point represents the normalized motility of each one of the 4 wells for the two conditions (with or without Na_2S). Different graphs correspond to the time point of 90 and 180 min of incubation. Welch test (90 min p = 1,83E-5) were performed, followed by Tukey´s pairwise test and Kruskal-Wallis test (115 min p = 3.5E-4 and 140 min p = 2.4E-4) followed by Dunn´s *post hoc*. Diamonds indicate statistical differences for each strain between sulfide and their control without sulfide. *C*, percentage of alive worms exposed to 1.5 mM of Na_2S solution (50 ppm of sulfide) for 3 or 20 h and then transferred to NGM plates with OP50 as food. Each data point represents the percentage of alive worms obtained in an independent experiment (∼50 animals per replicate were used). WT, wild-type N2 strain. Error bars represent the standard deviation. Kruskal-Wallis test was performed (Na_2S-3hs p = 6.3E-3 and Na_2S-20 hs p = 2.7E-3) and subsequent Dunn´s *post hoc* test. Asterisks indicate statistical difference (Na_2S-3hs *p = 1.4E-3 and Na_2S-20hs *p = 1.3E-3 and **p = 2.3E-2). *D*, gravid adults (24–30 h post L4) were exposed to a sulfide atmosphere (73 ppm) for 4 h, followed by 12 h of room air (RA) and the number of alive animals was scored. Each data point represents the percentage of alive worms obtained in an independent experiment (30 animals per replicate were used). WT, wild-type N2

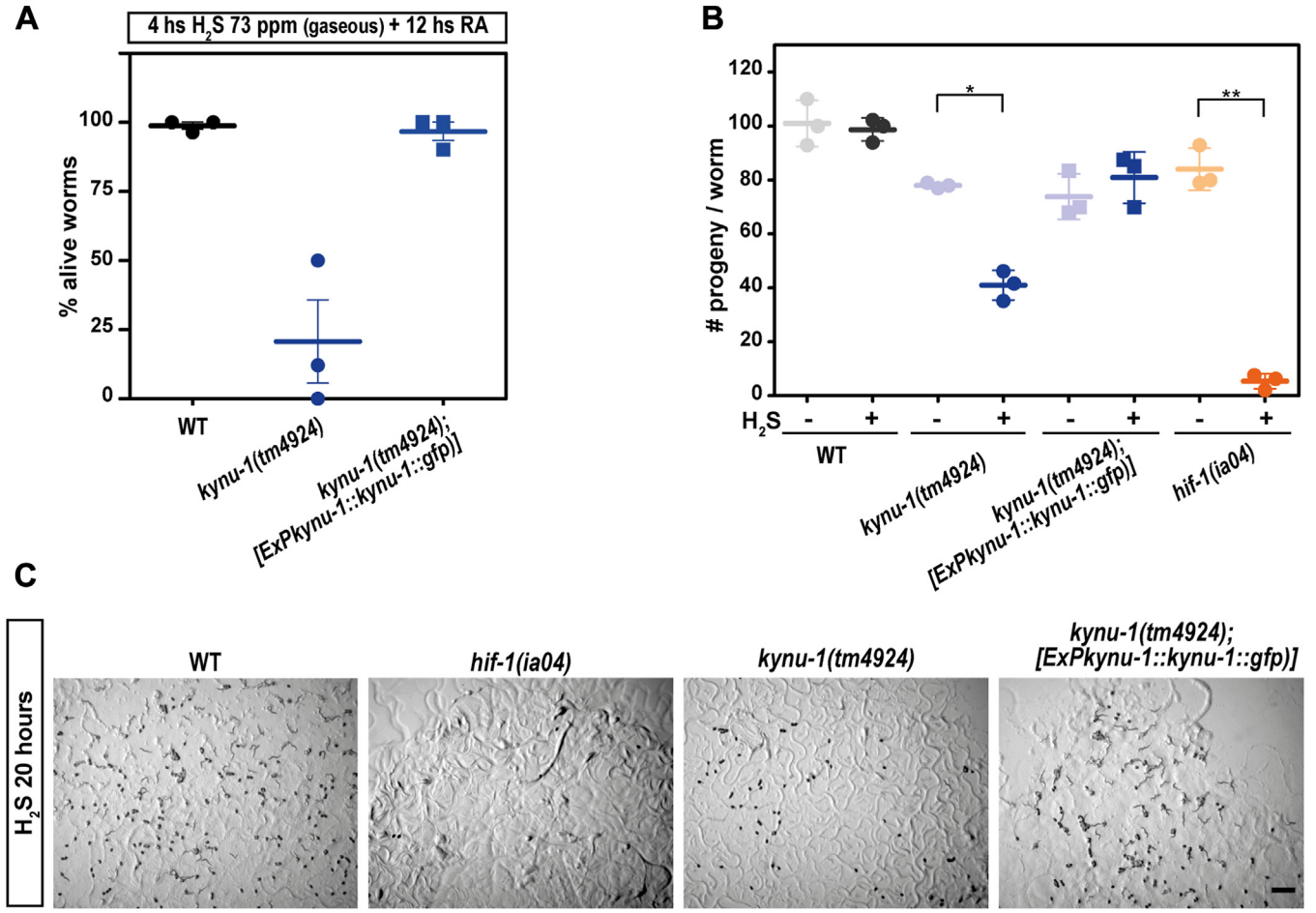

Figure 4. Sulfide affects survival and offspring size in the rhodoquinone-deficient mutant strain *kynu-1(tm4924)*. *A*, Gravid adults (24–30 h post L4) were exposed to a sulfide atmosphere (73 ppm) for 4 h, followed by 12 h of room air (RA) and the number of alive animals was scored. Each data point represents the percentage of alive worms obtained in an independent experiment (30 animals per replicate were used, three independent experiments). WT, wild-type N2 strain. Error bars represent the standard error of the mean. *B*, First-day adults were exposed to a sulfide atmosphere (+H_2S) or room air (−H_2S) for 20 h, and the number of progeny (embryos and L1) was scored. Each data point represents the mean of the number of offspring per adult worm obtained in an independent experiment (6 animals per condition per replicate were used). WT, wild-type N2 strain. Error bars represent the standard error of the mean. Means of three independent experiments are shown. ANOVA test was performed (p = 8.5E-11) and subsequently Tukey's pairwise test. Asterisks indicate statistical differences (*p = 9E-5 and **p = 5.6E-9). All the p values obtained with Tukey test are reported in Supporting information. *C*, representative images of the progeny of 6 adult worms after 20 h in the H_2S chamber of the following strains: wild-type N2, *kynu-1(tm4924), hif-1(ia04)* and *kynu-1(tm4924);ExPkynu-1::kynu-1::gfp*. Scale bar denote 500 µm. HIF-1 is required for the sulfide response and *hif-1(ia04)* mutant worms do not survive to 15 ppm of H_2S[11].

2Δ6e was slightly more sensitive to the PAO1 bacteria than the wild-type strain (Fig. S6). No difference was observed among the strains in the presence of the food bacterium *E. coli* OP50 (Fig. S7). These results highlight a putative role for RQ in the response to HCN-producing bacteria.

RQ-deficient mutant and wild-type strains are equally affected by paraquat stress

Ubiquinol, the reduced form of UQ, is a known lipid-soluble antioxidant for which there exist enzymic mechanisms that can regenerate its oxidized form, including SQRD/SQOR. In a halted ETC (*e.g.* cyanide and sulfide-rich conditions) ubiquinol cannot be regenerated. Alternative pathways might, therefore, enhance an organism's resistance to oxidative stress under such conditions, however it is unknown whether RQ can also function as an antioxidant, in a similar manner to UQ. In order to study a possible role of RQ in response to paraquat, the *kynu-1(tm4924)* mutant strain was exposed to this stressor, which among other outcomes generates reactive oxygen species mainly through a mechanism that involves complex I and cause cellular damage *via* lipid peroxidation (30). While the UQ-deficient mutant strain (*clk-1(qm30)*) was more sensitive to paraquat

strain. Error bars represent the standard error of the mean. Kruskal-Wallis test was performed (p = 5.7E-4) and subsequent Dunn´s *post hoc* test. Asterisks indicate statistical differences (*p = 1.2E-3 and **p = 5.6E-3). *E*, Motility assay (with *WMicrotracker*) using worm strains (*clk-1(qm30)* and WT) that were fed with the UQ-deficient bacteria *Escherichia coli* GD1 strain. Motility of *clk-1(qm30)* mutant and WT strains in the presence (+Na_2S) or absence (vehicle) of sodium sulfide (Na_2S) solution. The points indicate the average of the motilities of 6 wells relative to the motility measured only with vehicle, every 5 min for 300 min. The graph corresponds to a representative experiment with 6 wells per condition per strain (approximately 80 worms per well). Error bars indicate the standard deviation. Three biological replicates were performed with similar results (raw data included in Supporting information).

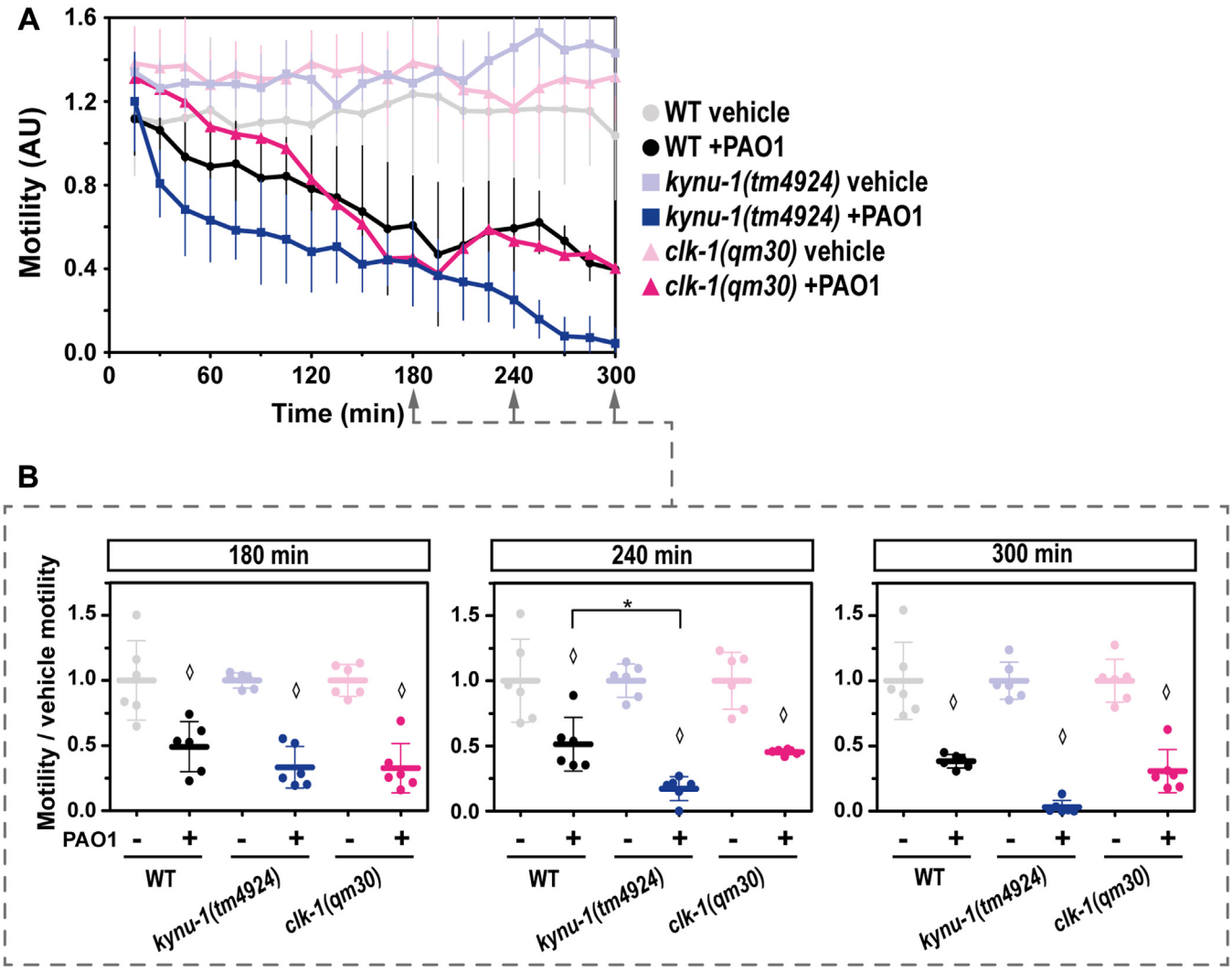

Figure 5. The rhodoquinone-deficient mutant strain *kynu-1(tm4924)* is more sensitive to *Pseudomonas aeruginosa* PAO1 strain than the ubiquinone-deficient mutant strain (*clk-1(qm30)*). The motility parameter refers to the movement of a population of individuals in liquid media and was measured using the infrared tracking device *WMicrotracker*. *A*, Motility of *kynu-1(tm4924)* and *clk-1(qm30)* mutants and wild-type (WT) strains in the presence (+PAO1) or absence (vehicle) of a liquid culture of *Pseudomonas aeruginosa* PAO1. Each point indicates the motility average of 4 wells (relative to the habituation, see methods) measured every 15 min for 300 min. The graph corresponds to a representative experiment with 6 wells per condition per strain (approximately 80 worms per well). Error bars indicate the standard deviation. At least three biological replicates were performed for each worm strain (all the replicates and raw data are included in Supporting information). *B*, For each strain (*kynu-1(tm4924)*, *clk-1(qm30)* and WT), the motility in the presence (+) or absence (–) of *P. aeruginosa* PAO1 was normalized to the mean of the motility in the absence of the bacteria. Each data point represents the normalized motility of each one of the 6 wells for the two conditions (with or without bacteria). Different graphs correspond to the time point of 180, 240, and 300 min of incubation. ANOVA test (180min p = 9E-9) and Welch test (240 min p = 7,4E-7) were performed, followed by Tukey´s pairwise test. Kruskal-Wallis test (300 min p = 1,7E-5) were performed, followed by Dunn´s *post hoc* test. The asterisk indicates statistical differences (*p = 0,04). Diamonds indicate statistical differences for each strain between the two conditions (bacteria and vehicle). All the p values obtained with different statistic tests are reported in Supporting information.

than the WT strain (Fig. 6), the RQ-deficient mutant strain was not, and showed a similar profile to the WT strain in response to paraquat.

Discussion

RQ is a lipidic electron carrier of an alternative mitochondrial ETC that constitutes a biochemical adaptation present in some animal lineages that face hypoxia (such as helminths, mollusks, and *C. elegans*) (19, 20). In this study, we demonstrate that the RQ-dependent ETC also serves a key role in an RQ-dependent sulfide oxidation pathway essential for sulfide detoxification.

In order to determine the role of RQ in sulfide *C. elegans* survival, we tested mutant strains unable to synthesize RQ (*kynu-1(tm4924)* and *coq-2(Δ6e)* strains (23, 28)) in the presence of sulfide. The two RQ-deficient mutant strains were highly sensitive to H_2S. Indeed, RQ-less and UQ-plus worms fed with OP50, a UQ-containing diet, did not recover from sulfide (Figs. 3 and S5). In contrast, UQ-less and RQ-plus worms (*clk-1(qm30)* and *coq-2(Δ6a)*) did recover from sulfide-rich conditions when fed with either UQ-plus or UQ-less bacterial diet (Figs. 3 and S5). This result indicates a more relevant role for RQ than UQ in worm survival under sulfide-rich conditions. The essentiality of RQ can be

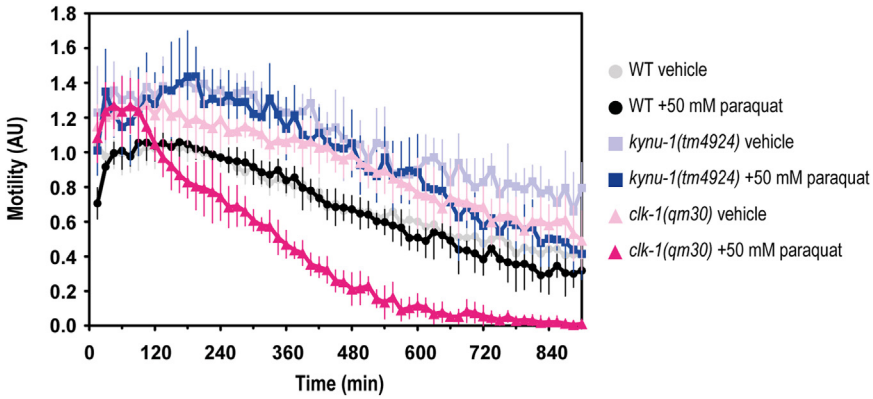

Figure 6. In contrast to the RQ-deficient mutant strain (*kynu-1(tm4924)*), the UQ-deficient mutant strain (*clk-1(qm30)*) was more sensitive to paraquat than the wild-type strain. The motility parameter refers to the movement of a population of individuals in liquid media and was measured using the infrared tracking device *WMicrotracker*. *A*, Motility of *kynu-1(tm4924)* and *clk-1(qm30)* mutants and wild-type (WT) strains in the presence (+paraquat) or absence (vehicle) 50 mM of paraquat. Each point indicates the motility average of 4 wells (relative to the habituation, see methods) measured every 15 min for 900 min. The graph corresponds to a representative experiment with 6 wells per condition per strain (approximately 80 worms per well). Error bars indicate the standard deviation. Three biological replicates with similar results were performed for each worm strain (all the replicates and raw data are included in Supporting information).

attributed to a functional sulfide alternative oxidation pathway. We propose the model depicted in Figure 7, contrasting the alternative sulfide oxidation ETC pathway with the canonical one. In this alternative ETC, SQRD oxidizes sulfide and reduces RQ, which in turn is regenerated by complex II which function as fumarate reductase, accepting electrons from reduced RQ. It is worth mentioning that it has been shown by Kumar, R. *et al.* 2022 (25) that mammalian complex II can function in reverse, oxidizing UQH2 to UQ allowing sulfide to be detoxified when complex IV is inhibited; yet, the standard redox potential of RQ would provide a much broader range of substrate concentrations to allow complex II to function as fumarate reductase.

Remarkably, mutants unable to synthesize RQ exhibited even greater sensitivity to sulfide compared to the *sqrd-1* mutant (Figs. 2 and 3). Because RQ can also accept electrons from complex I and transfer them to fumarate *via* complex II (Fig. 7*B*) it would also help to maintain ATP/ADP, NADH/NAD^+ and mitochondrial membrane potential homeostasis and to decrease the oxidative stress caused by a sulfide halted canonical ETC. Additional mechanisms of RQ contribution to sulfide detoxification and survival cannot be ruled out.

The results obtained with *kynu-1(tm4924)* mutant worms under paraquat stress do not reveal a direct role of RQ in response to the paraquat-generated oxidative stress (Fig. 6). However, since RQ would be part of sulfide oxidation pathway, these results cannot rule out a possible role of RQ in cellular redox homeostasis. The sulfide oxidation generates reactive sulfur species such as persulfides, polysulfides, and thiosulfate, which are involved in redox signaling and have a role in oxidant-antioxidant balance in cells (27). Specifically, through persulfidation and other post-translational modifications, these species contribute to protein protection against oxidation-induced aggregation (31, 32).

Another toxin commonly encountered by *C. elegans* in its natural environment is hydrogen cyanide produced by pathogenic bacterial strains that paralyze and kill the worm (10, 12). Similar to sulfur, cyanide also inhibits complex IV. Furthermore, RQ is essential for worm survival in cyanide (23). The mechanism proposed for HCN detoxification in the worm

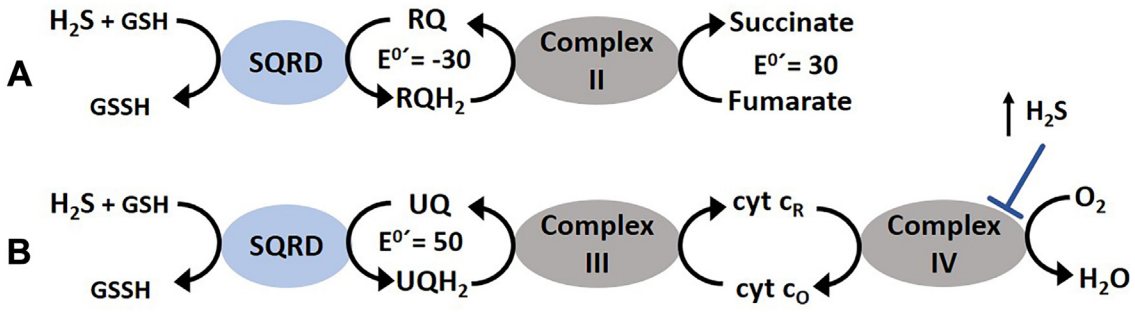

Figure 7. RQ- and UQ-dependent sulfide oxidation ETC. Based on our results, we propose the RQ-dependent model depicted *A*), contrasting the canonical sulfide oxidation ETC pathway depicted in *B*). In the alternative sulfide oxidation ETC, complex II functions as a fumarate reductase, allowing RQ to be recycled sustaining sulfide oxidation. Since complex IV is inhibited at high sulfide concentrations, this RQ-dependent pathway confers an advantage over the canonical pathway at toxic sulfide concentrations. Although it has been described that complex II can function as fumarate reductase with UQ, the standard reduction potential of RQH_2/RQ, lower than that of fumarate/succinate allows sulfide oxidation over a broader range of concentrations. The standard reduction $E^{0'}$ potential of rhodoquinone/rhodoquinol, ubiquinone/ubiquinol and fumarate/succinate are expressed in millivolts.

involves the enzyme CYSL-2 which consumes cyanide and generates H_2S. The H_2S produced triggers a recovery response to both chemicals and is detoxified mainly by the sulfide oxidation pathway (11). Importantly, the RQ-less mutant strain was slightly more sensitive to the cyanide-producing bacteria *P. aeruginosa* PAO1 than both the wild type and the UQ-less mutant strains (Figs. 5 and S6).

Interestingly, in contrast to mammals, *C. elegans* possess two SQRD/SQOR genes, *sqrd-1* and *sqrd-2*, the latter initially annotated as a pseudogen (quoted in (11)). However, we showed that *sqrd-2* is expressed in *C. elegans*. In concordance with our result, transcriptionally active regions of the *sqrd-2* gene were described in a tiling-array project run as part of the modENCODE initiative (33). Unlike the *sqrd-1* gene, *sqrd-2* does not change its expression under H_2S conditions according to microarray studies (16). On the other hand, RNAseq data obtained using strains that overexpress HIF-1 showed a 1.3-1.9-fold change in *sqrd-2* expression, suggesting regulation of *sqrd-2* expression in a HIF-1 dependent manner (34). Both SQRD-1 and SQRD-2 would be able to recognize RQ and UQ in their active sites; yet, the mutant strains exhibited different phenotypes in sulfide response. The *sqrd-1* mutant strain was more sensitive to sulfide than the wild-type N2 strain (Fig. 2), confirming its previously described role in sulfide detoxification (11). In contrast, the *sqrd-2* mutant strain recovered earlier than the wild-type strain, suggesting that SQRD-2 would function as a negative regulator as part of circuit that controls the sulfide response. It is interesting to note that *sqrd* gene duplication occurs in other animals that face sulfide and/or hypoxia (Fig. S1).

To sum up, we describe a new RQ function, key in the adaptive biochemical response to sulfide in *C. elegans*. Importantly, the alternative sulfide oxidation pathway described would confer an advantage in the presence of H_2S and HCN, and hence to pathogenic bacteria producing these toxins. More broadly, the animal lineages well-adapted to sulfide-rich environments (nematodes, annelids and bivalves) synthesize RQ. This reinforces the concept that RQ is a key biochemical adaptation not only for hypoxia but also for sulfide-rich environments.

Experimental procedures

Strains and culture conditions

General methods for *C. elegans* culture and maintenance were performed according to reference (35). All chemical reagents, unless otherwise specified, were purchased from Sigma-Aldrich-Merck. Table 2 lists the *C. elegans* strains used in this study, detailing the genotype and source. The *E. coli* OP50 strain used as *C. elegans* food was obtained from the *Caenorhabditis* Genetic Center (CGC). The *P. aeruginosa* PAO1 was kindly provided by Dr Colin Manoil (Universidad de Washington) and the ubiquinone-deficient *E. coli* strain GD1 was kindly provided by Dr Catherine Clarke (UCLA).

Sulfide solutions and quantification of the concentration

Crystals of $Na_2S{\cdot}9H_2O$ were stored in a desiccator until use. Solutions containing sulfide were prepared with ultrapure water in sealed vials. The sulfide concentration in solution was determined by the methylene blue colorimetric assay described in Siegel, L. M, 1964 (36) using an absorbance microplate reader Varioskan. The light path was determined as 0.58 cm for a 96 well plate and a total solution volume of 200 µl.

The gaseous H_2S for the sulfide chamber was generated using a solution of $Na_2S{\cdot}9H_2O$ in hydrochloric acid (1.31E-5 moles of Na_2S in 8 ml of HCl 50 mM for progeny assay and 6E-5 mol of Na_2S in 10 ml of HCl 50 mM) in a bohemian glass inside a chamber (1.44 L volume) and gentle stirring (40 rpm). The gaseous H_2S concentration was measured by the methylene blue method, mentioned above, extracting 2 ml of gas with a gas-tight Hamilton syringe and bubbling the gas in the alkaline zinc acetate solution of the assay. Using 1.31E-5 moles of Na_2S in 8 ml of HCl 50 mM, the H_2S concentration within the chamber reached 50 ppm within the first 3 h and then decayed over time (Fig. S3*D*).

Table 2
***C. elegans* strains used in this study, detailing the genotype and the source**

Strain	Genotype	Source
Bristol N2	Wild-type	CCG
TM3378	*sqrd-1 (tm3378) IV*	NBPJ
RB2485	*Y9C9A.16 (ok3440) IV*	CGC
TM4924	*kynu-1 (tm4924) X*	NBPJ
MQ130	*clk-1 (qm30) III*	CGC
IH25	*kynu-1 (tm4924)X; Ex [Pkynu-1::kynu1::gfp, pRF4]*	Institut Pasteur de Montevideo. Roberts Bucetta, P. *et al.*, 2019
PHX1715	*coq-2 (syb1715) III*	Suny Biotech Co., Ltd (Fuzhou City, China). Tan, J. H. *et al.*, 2020
PHX1721	*coq-2 (syb1721) III*	Suny Biotech Co., Ltd (Fuzhou City, China). Tan, J. H. *et al.*, 2020
ZG31	*hif-1 (ia4) V*	CGC

CGC: *Caenorhabditis* Genetic Center and NBPJ: *C. elegans* National Bioresource Project of Japan.

Toxicity tests using the tracking device WMicrotracker ONE

The toxicity test in liquid media was determined using the tracking device *WMicrotracker ONE* (PhylumTech, Argentina). The method used to determine worm motility is described in detail in (37). Briefly, the system detects motility through the interference of an array of infrared light beams, caused by worm movement. The readout is counts per unit of time (5 or 15 min in our experiments). Each count represents the interruption of the infrared light beam by worms. Experiments were performed in 96 well plates, using 80 to 100 synchronized L4 animals per well in a final volume of 100 µl. The number of worms used in this study falls within the linear range for motility *vs* worm number specified by the manufacturer instructions (https://www.phylumtech.com/home/en/linearity-curve-for-wmicrotracker-one-worms-per-well/). Six wells per condition per strain were used in each experiment (technical replicates). Experiments were repeated at least three times (biological replicates). In all cases, the counts per well at different times are normalized by the counts before adding the compound of interest or M9 buffer vehicle (basal counts or "habituation"). This normalization corrects the small differences that may exist in the number of worms per well. All the

assays included the wild-type strain and vehicle for each strain as controls.

For the experiments performed with GD1 as worm food, synchronized L1 larvae were placed in OP50 seeded NGM plates for 24 h and then washed three times in M9 and transferred to GD1 seeded NGM plates. The initial growth with OP50 is needed because *clk-1* worms fed on GD1 from L1 showed larval arrest. Because the different developmental time between the wild-type N2 and the *clk-1(qm30)* strains, the wild-type was incubated at 15 °C and the *clk-1* mutant at 20 °C until the motility assay. The *WMicrotracker* assays were performed using L4 worms.

Survival and progeny in sulfide atmosphere

For survival assays and progeny quantification, 24 to 30 h post-L4 adults *C. elegans* were placed on a 3-cm NGM plate seeded with OP50 bacteria. The plates were exposed to a H_2S in room air (RA) atmosphere for 20 h and survival was assessed immediately after removal from the H_2S/RA atmosphere. Animals were considered dead if they did not respond to tapping the plate or the worm touch with the wire pick. Additionally, after H_2S exposure, the number of eggs and larvae was scored in each plate. The maximal H_2S concentration obtained within the chamber was 50 ppm (see the section sulfide solutions and quantification of the concentration). For each strain, identical plates without sulfide (only RA) were included as controls. Experiments were conducted at 20 °C. The survival experiments in the sulfide chamber were performed during 4 h of incubation and the maximal sulfide concentration achieved was 75 ppm (see the section sulfide solutions and quantification of the concentration).

Statistical analysis

Normality and variance homogeneity were determined by Shapiro-Wilk and Levene´s tests, respectively, with a 5% significance level. Normal data were analyzed by ANOVA test and subsequent Tukey's test for pairwise comparisons. Samples with unequal variances were compared using the Welch F test and Tukey's test for pairwise comparisons. Non-parametric data were analyzed using the Kruskal-Wallis test and Dunn´s *post hoc* test for pairwise comparisons.

RNA isolation and Y9C9A.16 PCR amplification

RNA was extracted from ∼50-mg N2 worm pellets. For that 4000 synchronized L1s were grown on NGM plates at 20 °C to adulthood. For each experiment, ∼10,000 adult worms were harvested and washed three times with 18 megohm water to obtain pellets for extraction (∼50 mg) and frozen at −80 °C. The thawed pellet was ground in a Bullet Blender (Next Advance, USA) with 50 mg of zirconium oxide beads of 50 mm (Next Advance) for 2 min at power 8. Ground worms were used for RNA isolation using the QiAmp Viral RNA mini kit (Qiagen) according to the manufacturer's instructions. The RNA concentration was quantified using a NanoDrop spectrophotometer (Thermo Fisher Scientific) and the RNA was treated with a DNase I enzyme (Roche).

For the cDNA synthesis oligodT was used and the retrotranscription was performed using the Superscript IV reverse transcriptase (Thermo Fisher Scientific) enzyme. The PCR amplification of Y9C9A.16 gene fragment were performed using the specific primers gtcgacagttttcaagtgcg and ctcgaaaacttccaagtggc. The PCR amplification of *sqrd-1* gene fragment was performed using the specific primers tatggatgtggatggtggg and gccatcgtactgcatacatg, and for PCR amplification of *ama-1* fragment: ggagctcgagtggatcttcg and ttgtggagagtcggttgacg.

Homology modeling

SQRD-1 and SQRD-2 sequences were retrieved from Wormbase and a pdbBLAST search was performed in USCF ChimeraX (38). Human sulfide:quinone oxidoreductase (SQOR; pdb code 6OIB) was identified as the most similar sequence with its experimental structure determined (similarity 59%) and used as a template for homology modeling. Homology models were generated using Phyre2 (39), Swiss-model, Modeller (40), iTasser (41) and MOE (42). An energy minimization was performed on all models using Amber14:-EHT (43) forcefield implemented in MOE. RMSD between the model and the template, QMean score (44) and visual inspection were used to assess the quality of the models generated. The MOE model was selected for docking experiments given its good QMean score and the better loop modeling.

Docking

We previously optimized a docking protocol in MOE for the Q site of *C. elegans* mitochondrial complex II (45). The same protocol was validated using the human SQOR (pdb code 6OIB) using the co-crystallized ligand (ubiquinone). The RMSD value between the docked and the co-crystallized ligand was 0.137 Å. The protocol was then applied for ubiquinone and rhodoquinone docking with *C. elegans* SQRD-1 and SQRD-2 models. GBVI and KDeep score functions were employed as binding energy estimators.

Molecular dynamics

The four complexes obtained from docking experiments (SQRD-1b:UQ, SQRD-1b:RQ, SQRD-2b:UQ and SQRD2b:RQ) and the template crystal 6OIC were prepared using the QwikMD module (46, 47) of VMD 1.9.4 with the default settings except for the duration of each production stage, which was increased to 5,000,000 steps (10 ns). Five production stage were concatenated to give a total simulation time of 50 ns for each complex and 6OIC. Atom typing and CHARMM (48) forcefield parameter assignation for hydrogen sulfide, FAD and quinones were performed using CGenFF (49) server. Calculations were run in the NAMD 3.0 (50) alpha version using CUDA acceleration in a PC with a 12th Gen Intel Core i5-12400 × 12 processor and an NVIDIA GeForce RTX 4080/PCIe/SSE2 GPU with Ubuntu 22.04 LTS as the operating system. VMD was used for structural analysis and visualization.

Paraquat assay

A 0.1 M methyl viologen dichloride hydrate solution was prepared in ultrapure water and was added to an equal volume of M9 buffer containing worms in a 96-well plate. Worm motility assays were performed using the *WMicrotracker ONE*.

P. aeruginosa *PAO1 assays*

P. aeruginosa were grown in King B medium described by Bio-Rad, supplemented with glycine (4.4 g/L) and $FeCl_3$ (100 μM) to promote cyanide production as described in (51). An overnight culture was diluted in the same medium to obtain the same OD (at 600 nm) than the *E. coli* OP50 culture used as control.

Data availability

All the raw data is available and can be shared upon request: Laura Romanelli-Cedrez, lromanelli@pasteur.edu.uy or Gustavo Salinas, gsalin@fq.edu.uy.

Supporting information—This article contains supporting information (36).

Acknowledgments—We would like to thank Dr Ernesto Cuevasanta (Laboratorio de Fisicoquímica Biológica, Facultad de Ciencias, Universidad de la República, Uruguay) for technical assistance in sulfide determination; *Caenorhabditis* Genetic Center (CGC) for *C. elegans* mutant strains; Dr Colin Manoil (Universidad de Washington, USA) and Dr Catherine Clarke (UCLA, USA) for *P. aeruginosa* and *E. coli* strains.

Author contribution—G. S. and L. R-C. conceptualization; G. S. and L. R-C. funding acquisition; G. S. project administration; G. S. resources; G. S. supervision; G. S., F. V., and L. R-C. writing–original draft; G. S., F. V., and L. R-C. writing–review & editing; G. S., F. V., and L. R-C. formal analysis; F. V. and L. R-C. investigation; F. V. and L. R-C. methodology; L. R-C. project administration.

Funding and additional information—ANII agency (FCE_3_2020_1_162629 to L.R.) and FOCEM - Fondo para la Convergencia Estructural del Mercosur (COF 03/11 to G.S.).

Conflict of interest—The authors declare that they have no conflicts of interest with the contents of this article.

Abbreviations—The abbreviations used are: H2S, Hydrogen sulfide; RQ, rhodoquinone; SQOR, sulfide-quinone oxidoreductase; UQ, ubiquinone.

References

1. Nicholls, P., and Kim, J. K. (1982) Sulphide as an inhibitor and electron donor for the cytochrome c oxidase system. *Can. J. Biochem.* **60**, 613–623
2. Filipovic, M. R., Zivanovic, J., Alvarez, B., and Banerjee, R. (2018) Chemical biology of H2S signaling through persulfidation. *Chem. Rev.* **118**, 1253–1337
3. Bailly, X., and Vinogradov, S. (2005) The sulfide binding function of annelid hemoglobins: relic of an old biosystem? *J. Inorg. Biochem.* **99**, 142–150
4. Broman, E., Bonaglia, S., Holovachov, O., Marzocchi, U., Hall, P. O. J., and Nascimento, F. J. A. (2020) Uncovering diversity and metabolic spectrum of animals in dead zone sediments. *Commun. Biol.* **3**, 1–12
5. Sun, Y., Wang, M., Zhong, Z., Chen, H., Wang, H., Zhou, L., *et al.* (2022) Adaption to hydrogen sulfide-rich environments: strategies for active detoxification in deep-sea symbiotic mussels, Gigantidas platifrons. *Sci. Total Environ.* **804**, 150054
6. Salinas, G., Langelaan, D. N., and Shepherd, J. N. (2020) Rhodoquinone in bacteria and animals: two distinct pathways for biosynthesis of this key electron transporter used in anaerobic bioenergetics. *Biochim. Biophys. Acta* **1861**, 148278
7. Libiad, M., Yadav, P. K., Vitvitsky, V., Martinov, M., and Banerjee, R. (2014) Organization of the human mitochondrial hydrogen sulfide oxidation pathway. *J. Biol. Chem.* **289**, 30901–30910
8. Jackson, M. R., Melideo, S. L., and Jorns, M. S. (2012) Human sulfide: Quinone oxidoreductase catalyzes the first step in hydrogen sulfide metabolism and produces a sulfane sulfur metabolite. *Biochemistry* **51**, 6804–6815
9. Theissen, U., Hoffmeister, M., Grieshaber, M., and Martin, W. (2003) Single eubacterial origin of eukaryotic sulfide:quinone oxidoreductase, a mitochondrial enzyme conserved from the early evolution of eukaryotes during anoxic and sulfidic times. *Mol. Biol. Evol.* **20**, 1564–1574
10. Gallagher, L. A., and Manoil, C. (2001) Pseudomonas aeruginosa PAO1 kills Caenorhabditis elegans by cyanide poisoning. *J. Bact.* **183**, 6207–6214
11. Budde, M. W., and Roth, M. B. (2011) The response of caenorhabditis elegans to hydrogen sulfide and hydrogen cyanide. *Genetics* **189**, 521–532
12. Darby, C., Cosma, C. L., Thomas, J. H., and Manoil, C. (1999) Lethal paralysis of Caenorhabditis elegans by Pseudomonas aeruginosa. *Proc. Natl. Acad. Sci. U. S. A.* **96**, 15202–15207
13. Wang, B., Pandey, T., Long, Y., Delgado-Rodriguez, S. E., Daugherty, M. D., and Ma, D. K. (2022) Co-opted genes of algal origin protect C. elegans against cyanogenic toxins. *Curr. Biol.* **32**, 4941–4948.e3
14. Ma, D. K., Vozdek, R., Bhatla, N., and Horvitz, H. R. (2012) CYSL-1 interacts with the O 2-sensing hydroxylase EGL-9 to promote H 2S-modulated hypoxia-induced behavioral plasticity in C. elegans. *Neuron* **73**, 925–940
15. Vozdek, R., Hnízda, A., Krijt, J., Šerá, L., and Kožich, V. (2013) Biochemical properties of nematode O-acetylserine(thiol)lyase paralogs imply their distinct roles in hydrogen sulfide homeostasis. *Biochim. Biophys. Acta* **1834**, 2691–2701
16. Miller, D. L., Budde, M. W., and Roth, M. B. (2011) HIF-1 and SKN-1 coordinate the transcriptional response to hydrogen sulfide in Caenorhabditis elegans. *PLoS One* **6**, e25476
17. Budde, M. W., and Roth, M. B. (2010) Hydrogen Sulfide Increases Hypoxia-Inducible Factor-1 Activity Independently of von Hippel-Lindau Tumor Suppressor-1 in C. elegans. *Mol. Biol. Cell.* **21**, 212–217
18. Horsman, J. W., Heinis, F. I., and Miller, D. L. (2019) A novel mechanism to prevent H2S toxicity in caenorhabditis elegans. *Genetics* **213**, 481–490
19. Sato, M., and Ozawa, H. (1969) Occurrence of ubiquinone and rhodoquinone in parasitic nematodes, metastrongylus elongatus and Ascaris lumbricoides va.suis. *J. Biochem.* **65**, 861–867
20. Allen, P. C. (1973) Helminths: Comparison of their rhodoquinone. *Exp. Parasitol.* **34**, 211–219
21. Tielens, A. G. M., and Van Hellemond, J. J. (1998) The electron transport chain in anaerobically functioning eukaryotes. *Biochim. Biophys. Acta* **1365**, 71–78
22. Van Hellemond, J. J., Klockiewicz, M., Gaasenbeek, C. P. H., Roos, M. H., and Tielensi, A. G. M. (1995) Rhodoquinone and complex II of the electron transport chain in anaerobically functioning eukaryotes. *J. Biol. Chem.* **270**, 31065–31070
23. Del Borrello, S., Lautens, M., Dolan, K., Tan, J. H., Davie, T., Schertzberg, M., *et al.* (2019) Rhodoquinone biosynthesis in 1 C.elegans requires precursors generated by the kynurenine pathway. *Elife* **8**, 1–21
24. Erabi, T., Higuti, T., Tomisaburo KAKUNO, -l, Yamashita, J., Tanaka, M., and Horio, T. (1975) Polarographic studies on ubiquinone-10 and rhodoquinone bound with chromatophores from rhodospirillum rubrum. *J. Biochem.* **78**, 795–801

25. Kumar, R., Landry, A. P., Guha, A., Vitvitsky, V., Lee, H. J., Seike, K., *et al.* (2022) A redox cycle with complex II prioritizes sulfide quinone oxidoreductase dependent H2S oxidation. *J. Biol. Chem.* **298**, 101435
26. Mishanina, T. V., Yadav, P. K., Ballou, D. P., and Banerjee, R. (2015) Transient kinetic analysis of hydrogen sulfide oxidation catalyzed by human sulfide quinone oxidoreductase. *J. Biol. Chem.* **290**, 25072–25080
27. Mishanina, T. V., Libiad, M., and Banerjee, R. (2015) Biogenesis of reactive sulfur species for signaling by hydrogen sulfide oxidation pathways. *Nat. Chem. Biol.* **11**, 457–464
28. Roberts Buceta, P. M., Romanelli-Cedrez, L., Babcock, S. J., Xun, H., VonPaige, M. L., Higley, T. W., *et al.* (2019) The kynurenine pathway is essential for rhodoquinone biosynthesis in Caenorhabditis elegans. *J. Biol. Chem.* **294**, 11047–11053
29. [preprint] Tan, J. H., Lautens, M., Romanelli-Cedrez, L., Wang, J., Schertzberg, M. R., Reinl, S. R., *et al.* (2020) Alternative splicing of COQ-2 determines the choice between ubiquinone and rhodoquinone biosynthesis in helminths. *bioRxiv*. https://doi.org/10.1101/2020.02.28.965087
30. Cochemé, H. M., and Murphy, M. P. (2008) Complex I is the major site of mitochondrial superoxide production by paraquat. *J. Biol. Chem.* **283**, 1786–1798
31. Zivanovic, J., Kouroussis, E., Kohl, J. B., Adhikari, B., Bursac, B., Schott-Roux, S., *et al.* (2019) Selective persulfide detection reveals evolutionarily conserved antiaging effects of S-Sulfhydration. *Cell Metab.* **30**, 1152–1170.e13
32. Dóka, Ida. T., Dagnell, M., Abiko, Y., Luong, N. C., Balog, N., Takata, T., *et al.* (2020) Control of protein function through oxidation and reduction of persulfidated states. *Sci. Adv.* **6**, eaax8358
33. Gerstein, M. B., Lu, Z. J., Van Nostrand, E. L., Cheng, C., Arshinoff, B. I., Liu, T., *et al.* (2011) Integrative analysis of the Caenorhabditis elegans genome by the modENCODE project. *Science* **330**, 1775–1787
34. Vora, M., Pyonteck, S. M., Popovitchenko, T., Matlack, T. L., Prashar, A., Kane, N. S., *et al.* (2022) The hypoxia response pathway promotes PEP carboxykinase and gluconeogenesis in C. elegans. *Nat. Commun.* **13**, 6168
35. Sulston, J. E., and Hodgkin, J. (1997) Methods. In: Wood, W. B., ed. *The Nematode Caenorhabditis elegans (Cold Spring Harbor Monograph Series 17)*, 606, Cold Spring Harbor, Boulder: 587
36. Siegel, L. M. (1965) A direct microdetermination for sulfide. *Anal. Biochem.* **11**, 126–132
37. Simonetta, S. H., and Golombek, D. A. (2007) An automated tracking system for Caenorhabditis elegans locomotor behavior and circadian studies application. *J. Neurosci. Methods* **161**, 273–280
38. Pettersen, E. F., Goddard, T. D., Huang, C. C., Meng, E. C., Couch, G. S., Croll, T. I., *et al.* (2021) UCSF ChimeraX: structure visualization for researchers, educators, and developers. *Protein Sci.* **30**, 70–82
39. Kelley, L. a, Mezulis, S., Yates, C. M., Wass, M. N., and Sternberg, M. J. E. (2015) Europe PMC Funders Group the Phyre2 web portal for protein modelling , prediction and analysis. *Nat. Protoc.* **10**, 845–858
40. Kiefer, F., Arnold, K., Künzli, M., Bordoli, L., and Schwede, T. (2009) The SWISS-MODEL Repository and associated resources. *Nucleic Acids Res.* **37**, 387–392
41. Xiaogen, Z., Zheng, W., Li, Y., Pearce, R., Zhang, C., Bell, E. W., *et al.* (2022) I-TASSER-MTD: a deep-learning-based platform for multi-domain protein structure and function prediction. *Nat. Protoc.* **17**, 2326–2353
42. *Molecular Operating Environment (MOE), 2022.02.* (2022). Chemical Computing Group ULC, Montreal, QC
43. Case, D. A., Berryman, J. T., Betz, R. M., Cai, Q., Cerutti, D. S., Cheatham, T. E., III, *et al.* (2014) *The Amber Molecular Dynamics Package, Amber*, University of California, San Francisco, CA
44. Benkert, P., Tosatto, S. C. E., and Schomburg, D. (2008) QMEAN: a comprehensive scoring function for model quality assessment. *Proteins Struct. Funct. Genet.* **71**, 261–277
45. Vairoletti, F., Paulino, M., Mahler, G., Salinas, G., and Saiz, C. (2022) Structure-Based bioisosterism design, synthesis, biological evaluation and in silico studies of benzamide analogs as potential anthelmintics. *Molecules* **27**, 2659
46. Ribeiro, J. V., Bernardi, R. C., Rudack, T., Stone, J. E., Phillips, J. C., Freddolino, P. L., *et al.* (2016) QwikMD - integrative molecular dynamics toolkit for novices and experts. *Sci. Rep.* **6**, 1–14
47. Humphrey, W., Dalke, A., and Schulten, K. (1996) VMD: visual molecular dynamics. *J. Mol. Graph.* **14**, 33–38
48. Vanommeslaeghe, K., Hatcher, E., Acharya, C., Kundu, S., Zhong, S., Shim, J., *et al.* (2010) CHARMM General Force Field A Force Field for Drug-like Molecules Compatible with.Pdf. *J. Comput. Chem.* **31**, 671–690
49. Vanommeslaeghe, K., and Mackerell, A. D. J. (2012) Automation of the CHARMM general force field (CGenFF) I: bond perception and atom typing. *J. Chem. Inf. Model.* **52**, 3144–3154
50. Phillips, J. C., Hardy, D. J., Maia, J. D. C., Stone, J. E., Ribeiro, J. V., Bernardi, R. C., *et al.* (2020) Scalable molecular dynamics on CPU and GPU architectures with NAMD. *J. Chem. Phys.* **153**, 044130
51. Bakker, A. W., and Schippers, B. (1987) Microbial cyanide production in the rhizosphere in relation to potato yield reduction and Pseudomonas SPP-mediated plant growth-stimulation. *Soil Biol. Biochem.* **19**, 451–457